ELSEVIER

Biophysical Chemistry 50 (1994) 237–248

Biophysical Chemistry

Molecular dynamics study of the binding of phenylalanine stereoisomers to thermolysin

Indira Ghosh [a], Olle Edholm [b,*]

[a] *Astra Research Center India, 18th Cross Road, Malleswaram, Bangalore, 560 003 India*
[b] *Department of Theoretical Physics, Royal Institute of Technology, S-100 44 Stockholm 70, Sweden*

(Received 20 October 1993; accepted 1 December 1993)

Abstract

The stereospecificity in binding of phenylalanine as inhibitor in the active site of the thermolysin, has been investigated by means of molecular dynamics simulations using free energy integration techniques. The difference in the free energy of binding was found to be 2.0 ± 1.8 kJ/mol in favour of the D-form. This agrees with the experimental value, 2.8 kJ/mol. The result was obtained using a standard empirical force field (that of GROMOS). A different force field with 30% bigger charges (more like ab initio charges) was also tried. This resulted in less fluctuations and a more precise binding, but in a free energy difference that was clearly larger than the experimental one. The phenylalanine backbone is located close to the zinc atom and the ring stays in the hydrophobic pocket in both the cases. The two stereoisomers differ mainly in the orientation of the backbone plane with respect to the active site and the rotational state of the dihedral around the C^{α}–C^{β} bond.

Key words: Computer simulation; Cyclic perturbation; Thermodynamic integration; Free energy difference; Stereomers; Active site; Enzyme–inhibitor interaction

1. Introduction

Stereospecificity is an important property of many enzymes involved in the catalysis of the reactions in the living cell. This stereoselectivity is necessary, since many of the building blocks of cells as amino acids, nucleic acids and carbohydrates do only occur in one of the two isomeric forms (L or D) in the living organisms while they occur in both forms in nature. Thus, a stereo specific recognition is required in many of the chemical reactions occurring in the cell metabolism. Most enzymes do in fact accurately select between the two stereoisomers. For instance, the hydrolytic proteases α-chymotrypsin, thermolysin and pepsin digest L-amino acid containing substrates, but has no effect on D containing ones [1–3]. All of them bind both L- and D-amino acids as inhibitors, although the binding constants differ significantly. It is generally assumed that both types of amino acids bind in a similar way by weak noncovalent interactions, in the active sites of these enzymes. The difference in three-dimensional structure does, however, affect the orientation and position of the inhibitor as well as details in the conformation of the

* Corresponding author.

SSDI 0301-4622(93)E0098-P

active site. This causes the differences in their interaction energies and binding constants. This may be studied in a classical framework using molecular dynamics simulations, energy minimizations or just energy calculations as a function of orientation and position of the substrate.

X-ray crystallographic studies of the binding of peptide inhibitors to thermolysin [4] show that they are able to bind in two different ways in the active site. The peptide bond of the inhibitor may either be parallel or antiparallel to the active site peptide chain. Considering the distance from the scissile peptide bond of the substrate to the zinc atom and other catalytic groups in the active site, these two modes of binding are refered to as "substrate" and "inhibitor" mode, respectively.

Here we will study the binding of L-Phe and D-Phe in the active site of thermolysin. This has earlier been done [5] using a rigid X-ray structure, allowing only for rotation of the substrate. These studies showed that energetically the L-isomer prefers to bind in the substrate mode and the D-isomer in the inhibitor. The present study differs by allowing flexibility for the substrate and the active site of the protein. We also include the solvent and will calculate the free energy difference of binding. The studies using molecular mechanics [6] on α-chymotrypsin suggest that flexibility of the protein and interaction with the solvent play important roles for the stereo-selectivity of that enzyme. The binding of substrate analogues to thermolysin have also been studied using molecular dynamics to elucidate the mechanism of binding and activity [7,8]. Here we study the reasons for the stereoselectivity of the active site of thermolysin and to find the reasons for different mode of binding for different isomers and their effect in the strength of binding. The binding of inhibitors to HIV protease has been considered by similar methods as those in this paper by [9,10].

For thermolysin, the preference of one isomer over the other in the formation of the inhibitor/protein complex has been observed and measured for a number of amino acids and dipeptides [2]. Here, we consider the binding of the two stereoisomers of phenylalanine in the active site of thermolysin. So, we have performed molecular dynamics simulations including thermolysin, inhibitor and water surrounding the active site. A free energy integration procedure has been used to calculate the difference in free energy of binding between the two isomers. From the bound structures obtained in these runs, we suggest a model for the difference in binding of the two stereoisomers.

Experimentally [2] the inhibition constants are 15.60×10^{-3} molar and 4.98×10^{-3} molar for L- and D-Phe, respectively. This means that the difference in binding energy is rather small, D-Phe is favored by only 2.8 kJ/mol. Further, the binding itself is weak with binding energies of 10.4 and 13.2 kJ/mol respectively. Because of the small difference in binding energy, we need an accuracy of the order of a kJ/mol in the simulations to obtain a significant result. This requires very long simulations and computing times. On the other hand, the small energy differences involved makes it easier to pass between the two states in reasonable computing times and the risk of getting trapped in metastable states is diminished. We have used a force field with the aliphatic hydrogens included in the carbon atoms into a united hydrocarbon group while the polar hydrogens are explicitly considered. This means that the L- and D-form of the amino acid just differs by the direction of the C^{α}–C^{β} bond relative to the backbone. An improper dihedral perturbation potential has been introduced that changes this direction continously between the two forms via the planar conformation.

2. Methodology

We consider the free energies in the following reaction scheme:

$$\begin{array}{ccc} \text{LPhe} + \text{water} + \text{tln} & \overset{\Delta G_{\text{L}}}{\rightleftharpoons} & [\text{tln} - \text{LPhe}]_{\text{aq}} \\ \Big\| \Delta G_{\text{aq}} = 0 & & \Big\| \Delta G_{\text{tln}} \\ \text{DPhe} + \text{water} + \text{tln} & \underset{\Delta G_{\text{D}}}{\rightleftharpoons} & [\text{tln} - \text{DPhe}]_{\text{aq}} \end{array} \qquad (1)$$

where ΔG_L and ΔG_D are the free energy changes in the actual reactions of binding the two isomers of phenylalanine to thermolysin, while ΔG_{aq} and ΔG_{tln} are those of two hypothetical reactions that convert the L-Phe into D-Phe in water solution respectively when bound to the enzyme. Since the total free energy change in a closed path is zero, the free energy difference that determines the preference for binding, $\Delta\Delta G = \Delta G_D - \Delta G_L$ can also be written:

$$\Delta\Delta G = \Delta G_D - \Delta G_L = \Delta G_{tln} - \Delta G_{aq}. \quad (2)$$

In experiments, the first expression is the useful one, while the latter one is more useful in computer simulations. The quantity ΔG_{tln} can be estimated using free energy integration techniques [11–13], while ΔG_{aq} is zero since the L- and D-forms of the amino acid dissolve equally well in water.

The free energy integration method has evolved as an efficient method to estimate differences in the free energy of binding between relatively similar molecules. It rests upon molecular dynamics simulations where one molecule is successively converted into the other form. This is done by adding a perturbing force into the simulations. This force depends upon a parameter λ that is zero in the initial state and one in the final state. In this case the perturbation is imposed by using an improper dihedral potential:,

$$E(\chi,\lambda) = C[\chi - (1-2\lambda)\chi_0]^2. \quad (3)$$

Here, χ is the improper dihedral that determines the angle between the C^α–C^β bond and the plane containing the N, C^α and carboxy-C atoms of the backbone of the Phe, C is the associated force constant and $\chi_0 = 35.264°$. The minimum of the potential varies from $+\chi_0$ to $-\chi_0$ during the conversion, where the extreme values correspond to the L- and D-forms of phenylalanine. Use of the united atom method i.e., inclusion of hydrogen in the C^α atom simplifies the conversion. The free energy difference $G(\lambda) - G(0)$ can be calculated as a function of λ from the expression

$$G(\lambda) - G(0) = \int_0^\lambda \langle \frac{\partial E}{\partial \chi} \rangle d\chi. \quad (4)$$

Obviously we are interested in $G(1) - G(0)$. We have used the slow growth method to do the conversion and changed λ linearly in time from zero to one in 20 ps.

One could also make use of a windowing techniques [14] instead of integration. We also tried that and did then sample at 10 discrete λ values for 1 ps. In between the λ values were changed and the system equilibrated. Half the computing time was then spent on sampling and half on changing λ and equilibrating. This gave consistent results that neither was significantly better or worse.

One could also imagine an alternate way to perform this conversion by changing the amino-group (NH_2) into a carboxy-group (COOH) and vice versa. We did test this but found that the conversion using the improper dihedral potential was the most convenient way to achieve the results in relatively short computing times.

When changing the improper dihedral potential it could be useful to change the minima of some angle potentials [15]. Otherwise one gets a large strain when the minimum of the improper dihedral potential is at zero and the valence angles at the C^α atom still correspond to a tetrahedral not planar geometry. A relaxation of the valence angle would remove a big part of the free energy maximum of about 20 kJ/mol close to $\lambda = 0.5$ seen in Fig. 3. This was not done in the actual simulations. The simulations are still correct although we think afterwards that a choice of this better reaction coordinate could at least slightly improve the results obtained in a given computing time or reduce the computing time necessary to obtain a given accuracy.

Thermolysin is a metallo-protease consisting of 316 amino acid residues having one zinc and four calcium atoms. The zinc atom forms three coordination bonds with the side chain atoms of the protein (N^ϵ of His146, N^ϵ of His142 and O^ϵ of Glu166) and one with a water oxygen. Its thermal stability is due to four calcium atoms, which do not participate directly in the activity of the protein. As suggested by X-ray structural studies [4], the active site of the protein lies around the zinc atom and a hydrophobic pocket containing the side chains of Val139, Leu133 and Ile188 and Leu202.

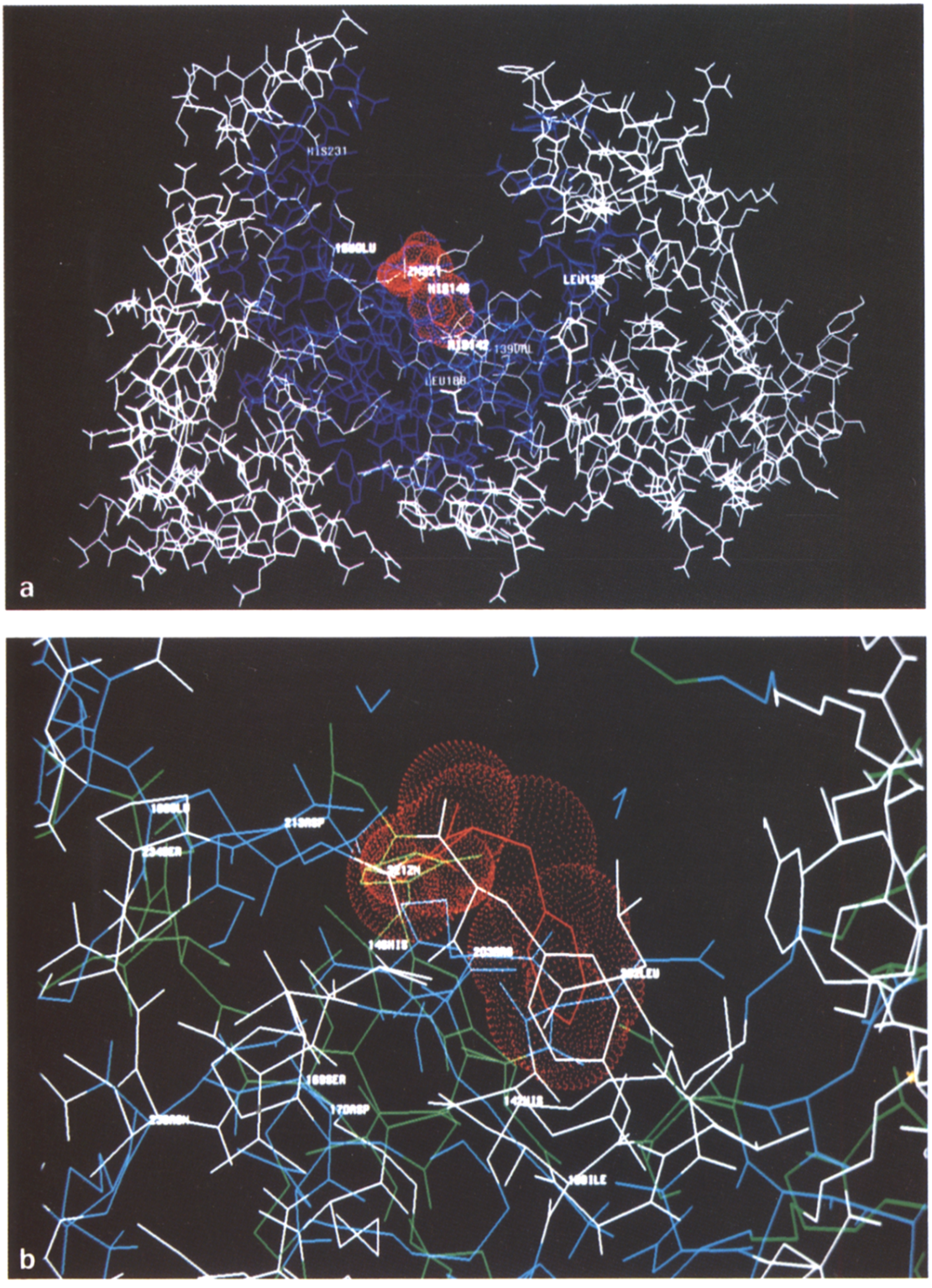

Fig. 1. Thermolysin and the inhibitor L-Phe at the active site. (a) The movable atoms are in colour blue and the L-Phe is shown with red dots. Rest of the protein is in white colour. (b) Active site residues with the inhibitor in red dots, hydrophobic residues in white, hydrophilic residues in blue and others in green. The pictures are generated on a Silicon Graphics workstation using the molecular graphics program HYDRA.

The initial configuration was prepared by starting from the crystal coordinates of thermolysin at 1.6 Å resolution [16] including some crystal water. The inhibitor, L-phenylalanine, was inserted into the active site and oriented using a rigid body rotation method [5] that eliminated short range contacts between inhibitor and protein. This complex was then incorporated into a cube consisting of 5832 equilibrated simple point charge (SPC) water [17]. Finally the water outside a sphere of 20 Å radius around the center of the active site was cut out. This center was determined as the middle point between the zinc atom and the C^{β} of the side chain of Val139. The total number of waters in this region around the active site was found to be 1168. This system was then energy minimized (100 steps steepest decent) and equilibrated for 5 ps with the protein atoms restrained to the crystal structure positions. The objective was to equilibrate the water at the protein surface to its new surroundings. In the final runs, all the protein atoms and waters inside a sphere of 12 Å radius around the center of the active site were allowed to move (Fig. 1) while the rest of the atoms were restrained to the positions in the equilibrated structure using a harmonic potential. The strength of the harmonic restraints were chosen to give average rms fluctuations of the protein atoms that were compatible with the experimental X-ray temperature factors [16] (Fig. 2). A list of the non-restrained protein residues (65 out of 316) and atoms is given in Table 1. A final 25 ps equilibration run was then performed on the entire system using these restraints before the free energy integration runs were started.

Table 1
List of mobile residues in thermolysin active site

Region number	Mobile residues	Mobile atoms
1	102–104	992–1015
2	110–149	1068–1426
3	157–192	1488–1827
4	201–203	1894–1927
5	226–235	2146–2229
6	319–322	2988–3005

The simulations were performed using the standard force field of GROMOS [17] with all amino acid residues neutral. This means that the side chains of the Glu:s, Asp:s, Arg:s and Lys:s have no net charges. This gives rise to electrostatic interactions at long ranges with no Coulomb part but only a dipole/dipole interaction as leading term. As water model we have used the single

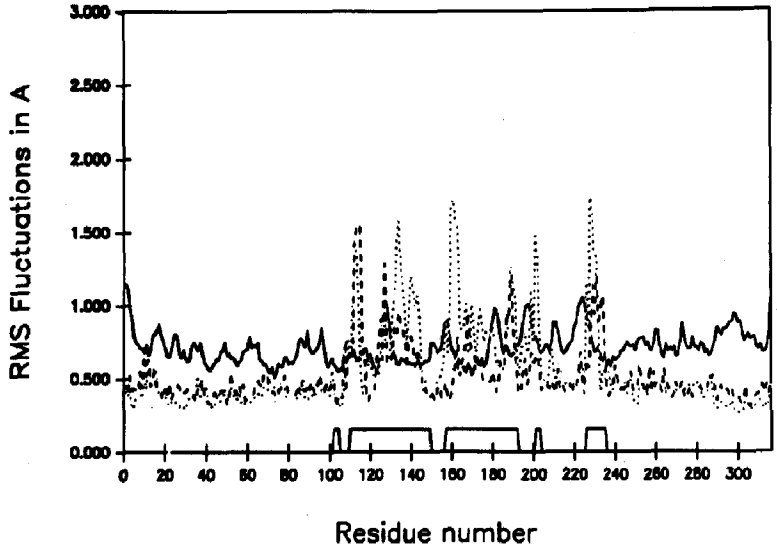

Fig. 2. R.M.S. fluctuation of C^{α} atoms of thermolysin in X-ray conformation (used *B*-factor) [13] (———), averaged over 320 ps. runs with normal charges (q-structures) (- - - - -), and averaged over 160 ps runs with 30% higher charges than GROMOS (·····).

point charge (SPC) water. The topology file created by GROMOS was modified for the zinc and calcium atoms to retain the coordination geometry with the ligands. The protein atoms coordinating with the metal atoms were treated as bonded to them with bond lengths and bond angles as found in the crystal structure [16]. With full positive charges on the metal atoms, we got distortions of the active site which have been observed by Merz and Kollman [8] earlier. Therefore, we used neutral zinc and calcium atoms, which resulted in a structure that was stable during the MD runs without any restraining of atoms in the active site. Bonded interactions were used to retain the coordination geometry of the zinc and calcium atoms close to that of the X-ray structure (compare Fig. 2) and keep the active site structure relaxed.

With these potential parameters, we got rather large fluctuations in the free energy change as well as in the position and orientation of the phenylalanine between different simulations. In an effort to make these fluctuations smaller, we made another series of runs with all the fractional charges increased by 30%, still keeping a zero net charge on all residues.

The interactions were cut off sharply (no switching function) at 12 Å. SHAKE [18] was used to restrain the bond lengths and a time step of 2 fs was used. To keep the temperature at 300 K, the system was coupled to a heat bath with a time constant of 0.1 ps [19]. The positional restraining force constant was 300 kJ/mol nm^2. A typical 20 ps integration run took 15 h clock time on an Alliant FX-2800 computer, when some of the most time consuming parts of the program were run in parallel over four processors.

For the L to D conversion in water we took the value zero for the free energy change ΔG_{aq}. To check the integration procedure, we did run a

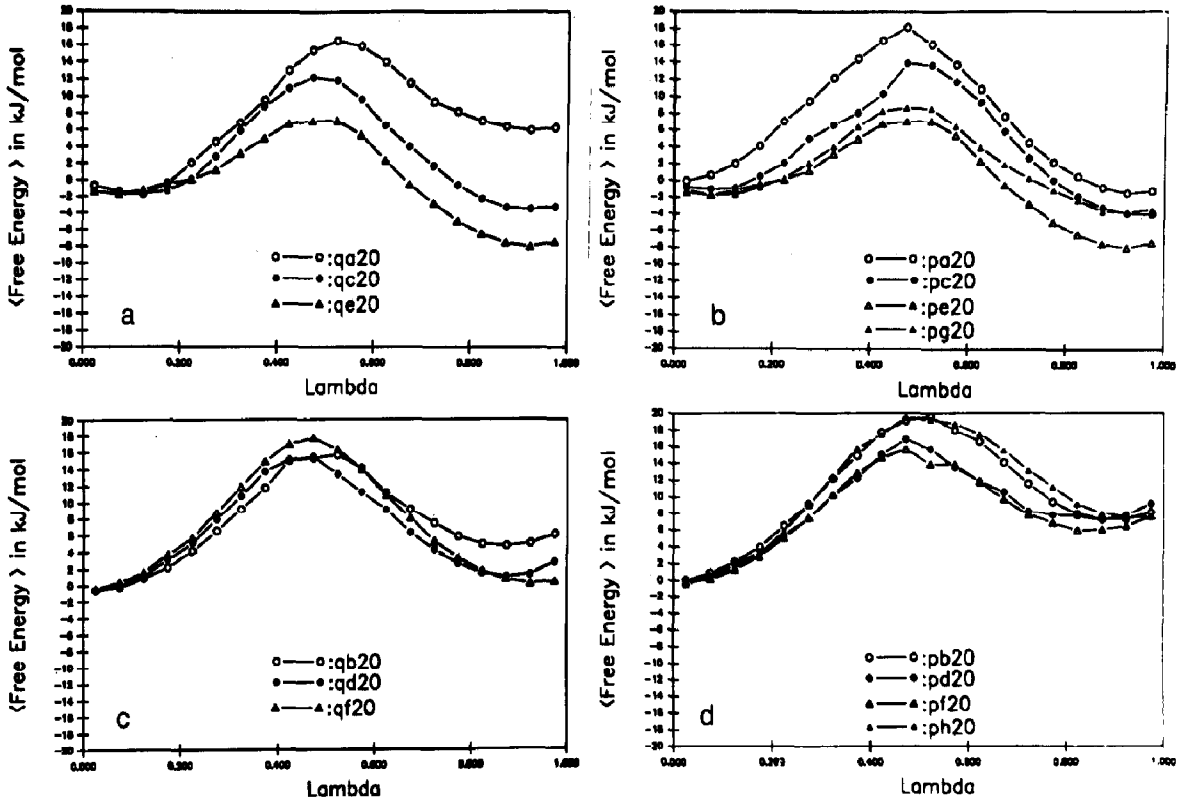

Fig. 3. Average free energy variation with lambda during the thermodynamic integration of 20 ps run in the case of normal charges during (a) L → D and (b) D → L conversions and 30% higher charges during (c) L → D and (d) D → L conversion.

Table 2
Free energy differences from the simulations

Normal charges		30% higher charges	
final conformations	$\langle\Delta\Delta G\rangle$ kJ/mol	final conformations	$\langle\Delta\Delta G\rangle$ kJ/mol
qa20(D)	+6.19	pa20(D)	−1.20
qb20(L)	+6.10	pb20(L)	+8.12
qc20(D)	−3.26	pc20(D)	−4.05
qd20(L)	+2.77	pd20(L)	+9.19
qe20(D)	+4.89	pe20(D)	−7.40
qf20(L)	+0.50	pf20(L)	+7.61
qa100(D) [a]	−1.40	pg20(D)	−3.49
qb100(L) [a]	+7.40	ph20(L)	+7.61
Average of all			
L → D	+0.9±4.1		−4.0±2.2
D → L	+4.9±2.7		+8.1±0.7
Final average [b]			
L → D	−2.0±1.8		−6.0±0.8

[a] These two simulations are over 100 ps and all the others are 20 ps.
[b] The error has been estimated by dividing the rms fluctuations with the square-root of the number of independent simulations.

couple of conversions of a system consisting of a periodic box with SPC-water and one dissolved phenylalanine. During the equilibration, the density was adjusted to give a pressure of about 1 atm. A series of 5 ps conversion runs gave a value of ΔG_{aq} that was less than 0.5 kJ/mol.

3. Results and discussion

The values of ΔG_{tln} from 16 simulations extending in total over 480 ps are shown in Table 2. Fig. 3 shows the free energy averaged over successive picoseconds as a function of the integration parameter λ during various 20 ps runs. It is essential to note that there is a systematic difference between the runs in the two directions. This hysteresis can be explained and predicted [15] and is not a measure of the inaccuracy of the method. For additional discussions of errors in free energy integrations see [20–23]. Therefore, the L to D and D to L integrations are averaged separately (with a $\sqrt{5}$ times higher wheight the 5 times longer 100 ps runs). The errror in the final estimate is found by dividing the standard deviation between the four runs in each direction with the square root of the number of independent runs.

As a final estimate we take the averages over the L to D and D to L runs with their appropriate signs. We then get a ΔG_{tln} value of −2.0 kJ/mol for the q series and −6.0 kJ/mol for the p series with the signs for the L to D transition. The non-systematic errors in these numbers are then estimated to ±1.8 kJ/mol and ±0.8 kJ/mol. In addition there is a systematic difference between the L to D and D to L conversions (hysteresis) of 2.9 and 2.0 kJ/mol repectively.

In a separate article [15], we have modeled this integration procedure by a Langevin equation along the reaction coordinate. There, it is shown that that we should expect a non-systematic error

$$2\sqrt{\frac{2\tau_c}{T}\Theta C\chi_0^2} \tag{5}$$

and a hysteresis

$$\frac{4\tau_c C\chi_0^2}{T}\left(\frac{C}{C+D}\right)^2. \tag{6}$$

Here, T is the simulation time (20 ps), Θ the absolute temperature times the Boltzmann constant (2.5 kJ/mol), τ_c the autocorrelation time of the random force (0.05 ps), C the force constant of Eq. (3) (340 kJ mol^{-1} rad^{-2}) and D the force constant of a harmonic mean force (Fig. 3 gives about −100 kJmol^{-1} rad^{-2}). These figures give about 2.5 kJ/mol both for the non-systematic errors and the hysteresis. This is in perfect agreement with the simulations.

The experimental value, −2.8 kJ/mol falls within the error limits of the final estimate for the q series, while it is clearly different from the result of the p series simulations. The simulations with the higher charges (p series) show relatively small fluctuations between different runs while those with normal charges (q series) do differ more. This indicates that the original charges give a more correct description of this system. When the charges are increased, we get a more precise binding with less fluctuations, but this occurs at the cost of more free energy to accommodate the L-form compared to the D-form.

Table 3
Average distances between the atoms of the phenylalanine and the protein active site

Inhibitor–active site	Distances (Å)	
	q20-structures	p20-structures
C-alpha-Zn	7.4±1.6	4.5±0.4
C-His142(ring)	7.1±1.2	4.0±0.2
N-His142(ring)	6.2±2.1	6.2±0.3
C-His146(ring)	10.4±1.1	5.4±0.5
N-His146(ring)	9.4±1.4	7.3±0.6
Phe-ring-Val139(CG:s)	5.5±0.6	varies [a]
Phe-ring-His231(ring)	19.3±1.7	varies [a]
Phe-ring-Zn	6.8±0.5	5.9±0.7

[a] See Fig. 5.

We now turn to a description of the structural changes that occur during the runs. For that we use distances between some important residues in thermolysin and the atoms in the phenylalanine. These are shown in Table 3. Further, the orientation of the backbone and the dihedral angle χ^1 ($N-C^{\alpha}-C^{\beta}-C^{\gamma}$) are important quantities to be discussed later.

In the structures from the runs with the higher charges (p series), the backbone of the phenylalanine stays fixed with the C^{α} close to the zinc and the carboxy group close to two of the zinc ligands, His142 and His146. The variation in these distances between the different p structures is only about 0.5 Å. The ring of the phenylalanine, on the contrary, changes its position during the simulations (Figs. 4 and 5). In the first two structures it remains in the hydrophobic pocket close to Val139 and Leu133. In the following simulations, it moves out of the pocket and over to the other side of the active site to the vicinity of His231. There, the ring only moves slightly back and forth during the following integration runs.

With normal charges, the backbone of the phenylalanine is less rigidly attached to the region of zinc, His142 and His146. This is seen in Table 3 as the distances to these residues are a couple of Å bigger than the corresponding distances in the p series of runs. Further, the fluctu-

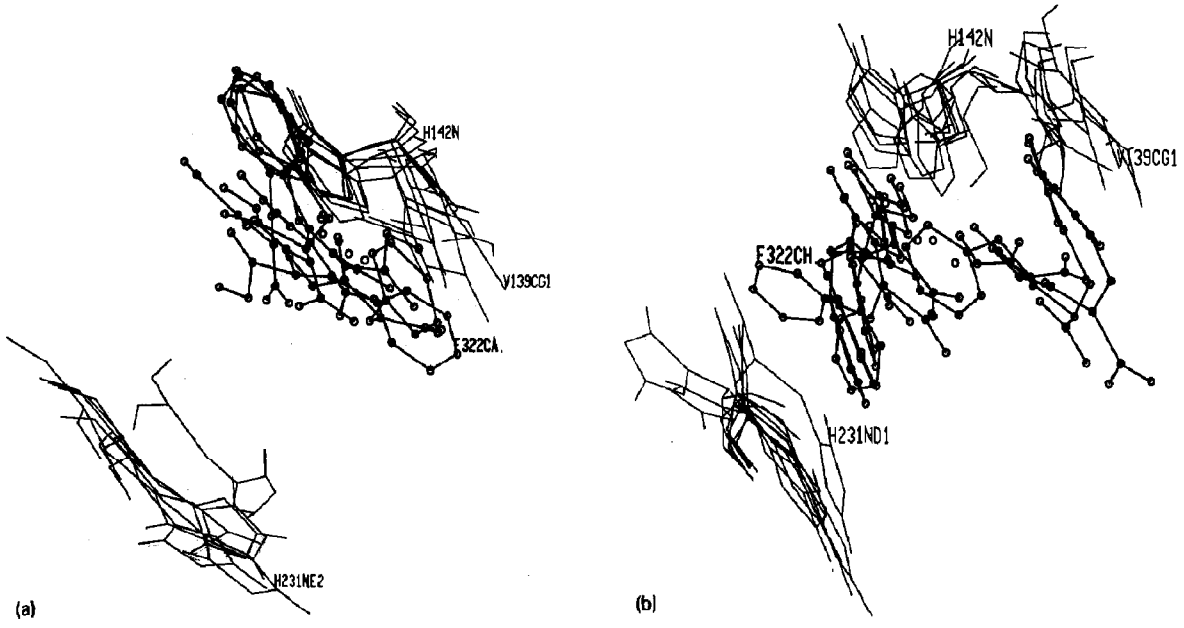

Fig. 4. A pictorial view of the important residues (Val-139, His-142 and His-231 in thin lines and zinc as a circle) of the active site of Thermolysin and the inhibitor (F322 (L or D) in thick lines with circles on the atoms). The final structures from all the thermodynamics integration runs for (a) normal charge i.e. q-series and (b) 30% higher charge i.e. p-series, are shown as superimpositions. A newly developed graphics program MOGRA [24] has been used.

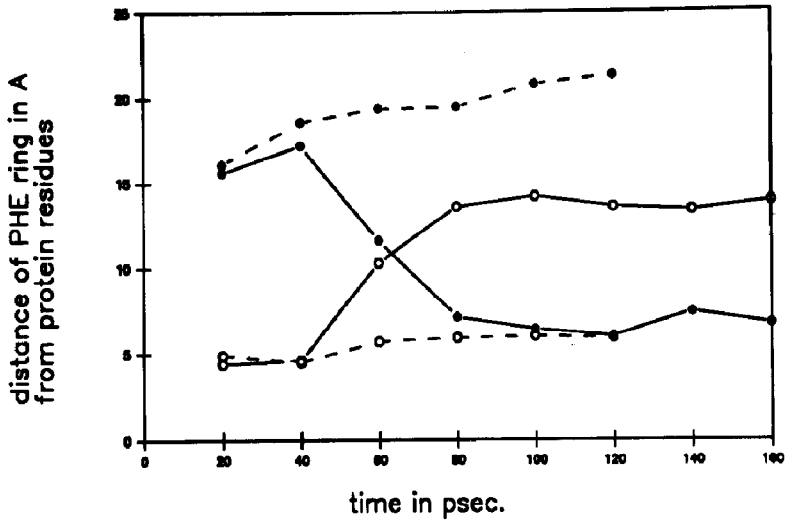

Fig. 5. The final distance of the centre of the phenylalanine ring to His-231 (●) and Val-139 (○) at the end of each conversion run has been plotted as a function of time in the normal charge i.e, q-series (- - - - -) and 30% higher charge i.e, p-series simulations (——).

ations in these distances between different structures are now 1–2 Å compared to 0.2–0.6 Å in the p series. This is a consequence of the weaker electrostatic interactions in the system with normal charges. The phenylalanine ring remains in this case in the hydrophobic pocket close to Val139 (Fig. 4a).

To describe the orientation of the phenylalanine backbone in the active site we may use two vectors, one connecting the carboxy- carbon and the nitrogen and the other one perpendicular to the backbone plane, C–C^{α}–N (Fig. 6). To compare the orientation in a series of structures we define two "order parameters" S_A and S_B associated with these vectors in the following way. The vectors are first normalized and then averaged over the series of structures. The length of the average vectors obtained in this way are taken as these order parameters. If the orientation of the phenylalanine is exactly the same in all structures, the order parameters will become 1. The more different the orientations of the phenylalanine ring are in the different structures, the closer will the order parameters be to 0.

From Table 4 it is seen that order parameter S_A is fairly close to one both for the q and p structures. This means that the C–N vector does

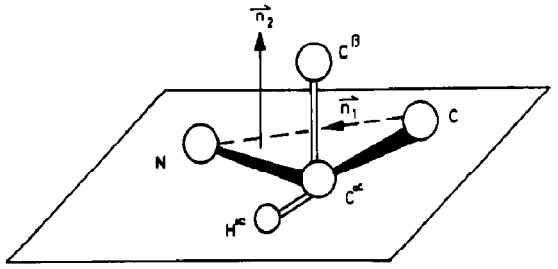

Fig. 6. A schematic representation of the vectors and the order parameters to define the orientation of the inhibitor at the active site. $S_A = |\Sigma n_1/m|$, $S_B = |\Sigma n_2/m|$, where m is the number of structures and n_1 and n_2 are the vectors.

Table 4
The order parameters S_A and S_B (as described in the text) calculated for normal and higher charged structures

Structures	S_A	S_B
qa20...qf20	0.78	0.29
qa20, qc20, qe20 (only D structures)	0.82	0.66
qb20, qd20, qf20 (only L structures)	0.73	0.79
pc20...ph20	0.83	0.67
pc20, pe20, pg20 (only D structures)	0.79	0.89
pd20, pf20, ph20 (only L structures)	0.97	0.95

not change orientation much during the integration runs. The S_B order parameter is much smaller, especially for the q structures. This indicates that the backbone plane has quite different orientation in the different structures. However, if S_B is calculated separately for the L- and D-conformations, we get values that are closer to one. This suggests that the stereoisomerization takes place by rotating the backbone plane 70° (as the L to D conversion is done by changing the improper dihedral angle from +35° to −35°) around the C–N vector. This means that the conversion occurs with the ring fixed in the hydrophobic pocket and without switching the carboxy- and amino-groups. Therefore, the free energy difference is small. Apparently, this mechanism faces difficulties when the charges are increased. The picture then becomes more complicated and the free energy difference increases.

The χ^1 dihedral angle (N–C^α–C^β–C^γ) is shown in Table 5 for the different structures. It lies close to the values at one of the minima of the dihedral potential at ±60° or 180° for all the structures. If the changes of this dihedral during the isomerizations are considered, one may see that the mechanism suggested previously is not sufficient to explain the phenomena. If the ring is kept fixed and the backbone is rotated 70° around the C–N vector to achieve the isomerization, the dihedral χ^1 will change with +60° for the L to D conversion and −60° for the opposite transition. This can be calculated by the three-dimensional geometry or more easily be seen from a molecular model. That rotation will bring the dihedral from a potential minimum up on the top of a barrier, which is clearly unfavorable. Therefore, the dihedral either remains in the initial well or makes an additional 60° rotation over to the next one. This is also what is seen from Table 5. For the L to D conversions we have $\Delta\chi^1$ approximately 0 or +120° while the change is 0 or −120° for the opposite transition. There is one exception, the pg20 to ph20 (D to L) conversion in which the dihedral changes with +126°. Then, the phenylalanine ring changes orientation considerably as seen from Fig. 4b.

4. Conclusions

Using molecular dynamics simulations with a standard force field, we have shown that the ring of both stereoisomers of phenylalanine may bind to thermolysin in the hydrophobic pocket containing Val139 and Leu133. The L- and D-forms of the amino acid are accommodated into this position having the backbones oriented differently. From eight separate thermodynamic integration runs, we deduce a difference in free energy of binding between the two stereoisomers of 2.0 ± 1.8 kJ/mol in favor of the D-form. This agrees with the experimental value 2.8 kJ/mol.

This change of backbone orientation does not alter the interactions very much, especially since there are some flexibility of the amino acids in the active site of thermolysin. Therefore, we get a very small free energy difference between the stereoisomers. However, when larger molecules as dipeptides like Gly–Phe bind, such a difference in backbone orientation would have a more

Table 5
Dihedral angle (in deg) χ^1 (N–C^α–C^β–C^γ) from the simulations

Structure	Normal charges		Conversion	Structure	30% higher charges	
	χ^1	$\Delta\chi^1$			χ^1	$\Delta\chi^1$
qa20(D)	62			pa20(D)	160	
qb20(L)	39	−23	(D → L)	pb20(L)	61	−99
qc20(D)	179	140	(L → D)	pc20(D)	160	99
qd20(L)	64	−115	(D → L)	pd20(L)	52	−108
qe20(D)	−163	133	(L → D)	pe20(D)	74	22
qf20(L)	−178	−15	(D → L)	pf20(L)	65	−9
			(L → D)	pg20(D)	74	9
			(D → L)	ph20(L)	−160	126

dramatic effect. Therefore, these molecules also have larger difference in free energy of binding (in favor of the D-form) than the single amino acids [2].

We also investigated a model in which the fractional charges of the force field were increased by 30%. The idea behind this was to bind the phenylalanine better in the active site close to the zinc-atom and His142 and reduce fluctuations in positions as well as free energies. We did achieve this objective. The phenylalanine backbone moved 2–3 Å closer into the active site, the positional fluctuations were reduced from 1–2 Å to less than 0.5 Å and the fluctuations in free energies were reduced by a factor 2. However, the difference in free energy of binding became 6.0 ± 0.8 kJ/mol clearly in disagreement with the experimental value. We did also get a motion of the ring away from the hydrophobic pocket into the vicinity of His231. This did, however, not affect the free energies.

Our conclusion is that the rather weak charges in the GROMOS model with the metal atoms treated as covalently linked at the active site estimates relative free energy of conversion of the inhibitors correctly. They allow a loose binding with fairly big fluctuations in positions as well as energies. This is necessary to accommodate both the L- and D-forms of the amino acid into the same position in the active site and still have a fairly small difference in free energy in agreement with experimental inhibition constants.

One could argue about how the electrostatics in the active site should be modeled. Certainly, a model with full charges on the metal atoms and the acidic and basic amino acids gives the wrong results. Then, not even the X-ray structure of the protein is stable. We have here taken the extreme opposite view, having no Coulomb interactions, just dipole/dipole interactions. Apparently this gives a weak enough binding of the inhibitor to reproduce the small free energy differences between the L- and D-forms. The trial with 30% higher charges on the dipoles indicates that one has to be careful with electrostatic interactions and that even slightly too big charges may result in wrong results. Apparently a modeling of the metal atoms without net charges, just stabilizing the protein with coordination bonds is sufficient to give a reasonable free energy difference for the binding of the two stereoisomers. To get correct absolute binding energies and a more accurate free energy difference between the stereoisomers, one would certainly have to use a more elaborate charge distribution in the active site region. Our results here indicate, however, that these charges have to be quite small. The general picture suggested here, with the aromatic ring bound in the hydrophobic pocket and the amino and carboxy ends of the amino acid pointing in approximately the same direction for the L- and D-form of the amino acid, may should hopefully still hold with such a more elaborate charge distribution. The difference between the steroisomers then lies in the orientation of the backbone plane and in the value of the first side chain dihedral.

Acknowledgement

We thank the Göran Gustafsson foundation for grants that has made some of IG's visits to Sweden possible. We thank the Swedish National Supercomputer Centre for some CRAY CPU time and OE thanks the Swedish National Research Council for support (grant K-KU-3777-107).

References

[1] E.C. Webb in: Symposium on the biochemical reactions of chemical warfare agents, ed. R.T. Williams, Biochem. Soc. Symp. No. 2 (1948) p. 50.
[2] J. Feder, L.R. Brougham and B.A. Wildi, Biochemistry 13 (1974) 1186.
[3] J.S. Fruton, Advan. Enzymol. 44 (1976) 1.
[4] W.R. Kester and B.W. Matthews, Biochemistry 16 (1977) 2506.
[5] I. Ghosh and V.S.R. Rao, J. Biom. Struct. Dyn. 2 (1984) 29.
[6] G. Wipff, A. Dearing, P.K. Weiner, J.M. Blaney and P.A. Kollman, J. Am. Chem. Soc. 105 (1983) 997.
[7] P.A. Bash, U.C. Singh, F.K. Brown, R. Langridge and P.A. Kollman, Science 235 (1987) 574.
[8] K.M. Merz Jr. and P.A. Kollman, J. Am. Chem. Soc. 111 (1989) 5649.

[9] A. Tropsha and J. Hermans, Protein Engineering 5 (1992) 29.
[10] D.M. Ferguson, R.J. Radmer and P.A. Kollman, J. Med. Chem. 34 (1991) 2654.
[11] W.F. van Gunsteren and P.K. Weiner, Computer simulation in biomolecular systems: theoretical and experimental applications (Escom, Leiden, 1989).
[12] B.L. Tembe and J.A. McCammon, Comput. Chem. 8 (1984) 281.
[13] C.F. Wong and J.A. McCammon J. Am. Chem. Soc. 108 (1986) 3830.
[14] D.A. Pearlman and P.A. Kollman, J. Chem. Phys. 90 (1989) 2460.
[15] O. Edholm and I. Ghosh, Mol. Sim. 10 (1993) 241.
[16] M.A. Holmes and B.W. Matthews, J. Mol. Biol. 160 (1982) 623.
[17] W.F. van Gunsteren and H.J.C. Berendsen, Groningen Molecular Simulation System (GROMOS).
[18] W.F. van Gunsteren and H.J.C. Berendsen, Mol. Phys. 34 (1977) 1311.
[19] H.J.C. Berendsen, J.P.M. Postma, W.F. van Gunsteren, A. Dinola and J.R. Haak, J. Chem. Phys. 81 (1984) 3684.
[20] T.P. Straatsma, H.J.C. Berendsen and A.J. Stam, Mol. Phys. 57 (1986) 89.
[21] R.H. Wood, J. Phys. Chem. 95 (1991) 4838.
[22] J. Hermans, J. Phys. Chem. 95 (1991) 9029.
[23] J. Hermans, R.H. Yun and A.G. Anderson, J. Comput. Chem. 13 (1992) 429.
[24] N.V. Ramana and I. Ghosh, Comput. Graph. 7 (1993) 415.